

The role of atomic chlorine in glacial-interglacial changes in the carbon-13 content of atmospheric methane

J. G. Levine, E. W. Wolff, A. E. Jones, and L. C. Sime

British Antarctic Survey, High Cross, Madingley Road, Cambridge, CB30ET, UK.

Abstract

The ice-core record of the carbon-13 content of atmospheric methane ($\delta^{13}\text{CH}_4$) has largely been used to constrain past changes in methane sources. The aim of this paper is to explore, for the first time, the contribution that changes in the strength of a minor methane sink—oxidation by atomic chlorine in the marine boundary layer (Cl_{MBL})—could make to changes in $\delta^{13}\text{CH}_4$ on glacial-interglacial timescales. Combining wind and temperature data from a variety of general circulation models with a simple formulation for the concentration of Cl_{MBL} , we find that changes in the strength of this sink, driven solely by changes in the atmospheric circulation, could have been responsible for changes in $\delta^{13}\text{CH}_4$ of the order of 10% of the glacial-interglacial difference observed. We thus highlight the need to quantify past changes in the strength of this sink, including those relating to changes in the sea-ice source of sea salt aerosol.

1. Introduction

Methane (CH_4) is an important atmospheric constituent on account of its potency as a greenhouse gas and its strong influence on the tropospheric oxidizing capacity. We know from the polar-ice record that between the last glacial maximum (LGM; 21 kyr before present (BP)) and the pre-industrial Holocene (PIH; 1 kyr BP) its concentration, $[\text{CH}_4]$, rose from around 360 ppbv to about

27 700 ppbv [e.g. Loulergue et al., 2008], but how much of this change was source-driven, and how
 28 much was sink-driven, remains uncertain [see, e.g., Valdes et al., 2005; Kaplan et al., 2006; Fischer
 29 et al., 2008]. This study focuses on the $^{12/13}\text{C}$ -isotopic composition of CH_4 trapped in polar ice,
 30 $\delta^{13}\text{CH}_4$, which provides a complementary constraint on the CH_4 budget and past changes therein
 31 [see, e.g., Ferretti et al., 2005; Fischer et al., 2008]. In the nomenclature of Schaefer and Whiticar
 32 [2008], $\delta^{13}\text{CH}_4$ can be expressed as the sum of the average isotopic composition of CH_4 sources,
 33 $\delta^{13}\text{C}_E$, and the average influence, by way of isotopic fractionation, of CH_4 sinks, ε_{WT} (equation 1).
 34 $\delta^{13}\text{C}_E$ can be broken down into the strength of each source, E_i , and its isotopic composition,
 35 $\delta^{13}\text{C}_{E_i}$ (equation 2). Similarly, ε_{WT} can be broken down into the fraction of CH_4 removed by each
 36 sink, F_j , and the fractionation coefficient associated with it, α_j (equation 3). Here, we explore the
 37 influence that CH_4 -oxidation by atomic chlorine in the marine boundary layer (Cl_{MBL}) has on
 38 $\delta^{13}\text{CH}_4$ (encapsulated by the term, $(\alpha_{\text{Cl}}-1).F_{\text{Cl}}$, in equation 3), specifically the contribution that
 39 changes in the strength of this sink could make to glacial-interglacial changes in $\delta^{13}\text{CH}_4$.

40

$$41 \quad \delta^{13}\text{CH}_4 = \delta^{13}\text{C}_E + \varepsilon_{WT} \quad (1)$$

$$42 \quad \delta^{13}\text{C}_E = \frac{\sum_{i=1}^n \delta^{13}\text{C}_{E_i} \cdot E_i}{\sum_{i=1}^n E_i} \quad (2)$$

$$43 \quad \varepsilon_{WT} = \sum_{j=1}^n (\alpha_j - 1) \cdot F_j \quad (3)$$

44

45 At present, about 80% of CH_4 is removed by the hydroxyl radical (OH) in the troposphere alone
 46 [e.g. Levy, 1971; Fung et al., 1991; Lelieveld et al., 1998]. Less than or similar to 10% is removed
 47 by soil uptake, and a similar fraction is removed by oxidants in the stratosphere [see, e.g., Fung et
 48 al., 1991; Lelieveld et al., 1998; Ridgwell et al., 1999]. It is estimated that Cl_{MBL} removes just 3-
 49 4% of CH_4 [e.g. Platt et al., 2004; Allan et al., 2007, 2010], yet owing to the strength of isotopic

50 fractionation associated with this sink ($\alpha_{Cl} > 1.06$ [e.g. Saueressig et al., 1995] c.f. $\alpha_{OH} = 1.0039$
51 [Saueressig et al., 2001] and $\alpha_{soil} = 1.017-1.025$ [e.g., Reeburgh et al., 1997; Snover and Quay,
52 2000]), Cl_{MBL} could be responsible for an enrichment in $\delta^{13}CH_4$ of 2.6‰ relative to $\delta^{13}C_E$ [Allan et
53 al., 2007]. Whilst changes in the strength of the Cl_{MBL} sink have been invoked to explain spatial
54 and inter-annual variations in $\delta^{13}CH_4$ [Allan et al., 2005, 2007], their potential to contribute to
55 glacial-interglacial changes has not been explored. Fischer et al. [2008], for example, did not
56 consider Cl_{MBL} when attempting to explain the 3.5‰ enrichment in $\delta^{13}CH_4$ they measured at the
57 LGM, relative to the pre-boreal Holocene (10 kyr BP). Schaefer and Whiticar [2008] did include
58 Cl_{MBL} in their study of the glacial-interglacial $\delta^{13}CH_4$ record, but did not allow for changes in the
59 strength of this sink. Here, we explore how sensitive the strength of the Cl_{MBL} sink is to a factor
60 that could well have changed on glacial-interglacial timescales: the horizontal wind speed at the sea
61 surface.

62
63 The main source of Cl_{MBL} is sea salt aerosol (SSA), which is produced by the action of the wind on
64 wave crests, and from which BrCl and Cl_2 (that photolyse to give Cl_{MBL}) are liberated [see, e.g.,
65 Vogt et al., 1996; Platt et al., 2004]. The abundance of SSA in pseudo steady-state is determined by
66 the rate of SSA production and the rate of SSA removal (e.g. by wet and dry deposition). The
67 abundance of Cl_{MBL} derived from SSA then depends on the abundance of SSA, the acidity of the
68 atmosphere, as BrCl and Cl_2 are believed to be liberated from SSA that has been acidified by the
69 products of dimethyl sulfide (DMS) oxidation [Vogt et al., 1996; Platt et al., 2004], and the
70 intensity of radiation of the wavelengths required to photolyse BrCl and Cl_2 . However, as a first
71 step in exploring the potential for Cl_{MBL} to contribute to glacial-interglacial changes in $\delta^{13}CH_4$, we
72 explore the influence of the circulation alone, on the grounds that the production of SSA is highly
73 sensitive to the wind speed [see, e.g., Monahan et al., 1986; Andreas et al., 1998; Witek et al.,
74 2007], and several lines of paleodata, including the ice-core records of dust and sea salt [e.g.

75 Thompson and Mosley-Thompson, 1981; Petit et al., 1981; Hansson, 1994; Rothlisberger et al.,
76 2002; and the recent review by Fischer et al., 2007], could indicate changes in this at the LGM.

77

78 We do so via a number of simple calculations employing a variety of model simulations of the PIH
79 and LGM circulations. It is important we explore a variety of simulations, as there has been little
80 consensus regarding the changes at the LGM, particularly in the region of the southern hemisphere
81 westerlies (SHW), with estimates ranging from a 40% reduction in surface wind speeds [Kim et al.,
82 2003] to a 25% increase in surface wind stress (implying a 12% increase in wind speeds) [Shin et
83 al, 2003] in this region. Much of the literature has focused on changes in the strength (and position)
84 of the SHW, owing to the bearing these could have on glacial-interglacial changes in CO₂ [see, e.g.,
85 Toggweiler, 1999; Toggweiler and Russell, 2008]. As the SHW exhibit some of the highest surface
86 wind speeds globally and cover a broad swath of the Southern Ocean (see Figure 1), changes in
87 their strength could also have bearing on the global strength of the Cl_{MBL} sink, and hence $\delta^{13}\text{CH}_4$.
88 By employing a variety of simulations, we probe the range of influences circulation-driven changes
89 in the strength of this sink could have had on $\delta^{13}\text{CH}_4$.

90

91

92 **2. Calculations**

93

94 We start by assuming that Cl_{MBL} removed the same fraction of CH₄ in the PIH as it is estimated to
95 remove in the present, and hence was responsible for an equal enrichment in $\delta^{13}\text{CH}_4$ (relative to
96 $\delta^{13}\text{C}_E$), namely 2.6(\pm 1.2)% [Allan et al., 2007]. We thus equate $(\alpha_{\text{Cl}}-1) \cdot F_{\text{Cl}}$, integrated seasonally
97 and globally in the PIH, to 2.6‰; see equation 3 and accompanying text. F_{Cl} is estimated to be
98 between 0.03 and 0.04 [Platt et al., 2004; Allan et al., 2007, 2010], hence F_{Cl} is small compared to
99 $1-F_{\text{Cl}}$ (the fraction of CH₄ removed by all other sinks) and a modest change in F_{Cl} , of up to say
100 \pm 50%, will have little effect on F_{OH} , F_{soil} etc. It follows that, to a good degree of approximation, an

101 X% increase (decrease) in $(\alpha_{Cl}-1).F_{Cl}$ will be accompanied by a 0.026X‰ enrichment (depletion) in
 102 $\delta^{13}CH_4$. Assuming the rate of CH_4 removal by each CH_4 sink is first order with respect to $[CH_4]$,
 103 and again as F_{Cl} is small compared to $1-F_{Cl}$, we assume F_{Cl} is proportional to the product of $[Cl_{MBL}]$
 104 and the rate coefficient for the reaction between Cl_{MBL} and CH_4 , k_{Cl} . Accordingly, an X% increase
 105 (decrease) in $(\alpha_{Cl}-1).k_{Cl}[Cl_{MBL}]$ will be accompanied by a 0.026X‰ enrichment (depletion) in
 106 $\delta^{13}CH_4$. We can calculate α_{Cl} according to equation 4 [Saueressig et al., 1995], and k_{Cl} (molecules⁻¹
 107 cm³ s⁻¹) according to equation 5 [Sander et al., 2003], where T is the temperature (K).

$$109 \quad \alpha_{Cl} = 1.043 \times e^{\frac{6.455}{T}} \quad (4)$$

$$110 \quad k_{Cl} = 9.6 \times 10^{-12} \cdot e^{\frac{-1360}{T}} \quad (5)$$

111
 112 To calculate $[Cl_{MBL}]$ (molecules cm⁻³), we use a modified version (our equation 7) of the simple
 113 formulation with which Allan et al. [2007] explored the role of Cl_{MBL} in spatial and inter-annual
 114 variations in $\delta^{13}CH_4$ (our equation 6). Equation 6 expresses $[Cl_{MBL}]$ in terms of an average
 115 concentration of 18×10^3 molecules cm⁻³ and a seasonal variation governed by the time of year, t
 116 (day number). The $\tanh(3\lambda)$ term, where λ is the latitude (radians), simply ensures the seasonal
 117 cycles in the northern and southern hemispheres are six months out of phase. To explore the
 118 influence that the wind has on $[Cl_{MBL}]$, we add a factor of $N.V^P$, where V is the horizontal wind
 119 speed (ms⁻¹), P is the power to which this is raised and N is a normalization factor, of which our
 120 results are independent as we are only interested in percentage changes in $[Cl_{MBL}]$. We do so on the
 121 basis that Gong et al. [2002] suggest the column loading of SSA is proportional to V^P (with P=1.39
 122 in the North Atlantic, 1.46 in the tropical Pacific, and 1.66 in the South Pacific). Assuming (1) the
 123 column loading of Cl_{MBL} is proportional to that of SSA, (2) the Cl_{MBL} is concentrated in the marine
 124 boundary layer (MBL), and (3) the height of the MBL does not change, $[Cl_{MBL}]$ should also be
 125 proportional to V^P . Though Gong et al. [2002] did not comment on it, their plots of loading versus

126 wind speed [their Figure 2] indicate a proportionality to $V^{3.41}$, or similar, at wind speeds above
127 about 5ms^{-1} . We therefore employ (globally) $P=1.39$ at $V\leq 5\text{ms}^{-1}$ and 3.41 at $V>5\text{ms}^{-1}$, but also
128 explore the sensitivity of our results to variations in this formulation (see later).

129

$$130 \quad [Cl_{MBL}] = 18 \times 10^3 \cdot \{1 + \tanh(3\lambda) \sin[2\pi(t - 90)/365]\} \quad (6)$$

131

$$132 \quad [Cl_{MBL}] = 18 \times 10^3 \cdot \{1 + \tanh(3\lambda) \sin[2\pi(t - 90)/365]\} \cdot N \cdot V^P \quad (7)$$

133

134 With equations 4, 5 and 7, we can calculate $(\alpha_{CI}-1) \cdot k_{CI}[Cl_{MBL}]$ as a function of season and location
135 during the PIH and LGM, provided we have the necessary wind and temperature data. Summarized
136 in Table 1, these are taken from simulations with five general circulation models, more information
137 on which can be found in our Auxiliary Material. Figure 1 illustrates the annual-mean surface wind
138 speeds and temperatures in the PIH, and the changes in these at the LGM, according to each model.
139 It also illustrates the percentage changes we calculate in $[Cl_{MBL}]$ at the LGM based on the wind
140 data. Subject to the data from each model, we calculate the seasonally and globally integrated value
141 of $(\alpha_{CI}-1) \cdot k_{CI}[Cl_{MBL}]$ throughout the MBL (treating areas of sea ice and open ocean alike; discussed
142 later) in both the PIH and LGM, and hence the percentage change in this quantity on switching from
143 PIH to LGM winds and temperatures, which we relate to a per-mil change in $\delta^{13}\text{CH}_4$.

144

145 We use mainly climatological monthly-mean data (based on 100-year integrations, or 20-year
146 integrations in the case of HadAM3), these being arguably the most robust. However, we also
147 repeat our calculations with CCSM3 and HadAM3 data, employing a full 100 years of monthly-
148 mean data and a full 20 years of daily-mean data, respectively, to explore the sensitivity of our
149 results to the degree of temporal averaging; see Table 1. To assess the sensitivity of our results to
150 our formulation for P , we repeat all of these ‘base’ calculations (B) subject to an alternative value of
151 P at $V\leq 5\text{ms}^{-1}$ (1.66; S1) and alternative values of V at which we switch from $P=1.39$ to $P=3.41$

152 (4ms⁻¹ in S2 and 6ms⁻¹ in S3). We also assess the sensitivity of our results to: the seasonality of
153 [C]_{MBL}, by repeating the base calculations with the tanh(3λ)sin[2π(t-90)/365] term in equation 7 set
154 to zero (S4); and the changes in temperature between the PIH and LGM, by changing the winds
155 whilst keeping the temperatures (PIH) constant (S5).

156

157

158 **3. Results**

159

160 The results of the base (B) and sensitivity (S1-5) calculations are given in Table 2; the numbers in
161 parentheses correspond to the results obtained when less ‘temporally averaged’ data are employed
162 (see Table 1 and accompanying text). We find that the effect on δ¹³CH₄ of switching from PIH to
163 LGM winds and temperatures depends on which model data we use and the degree to which these
164 are temporally averaged, with the base calculations yielding everything from a depletion of 0.46‰
165 to an enrichment of 0.14‰.

166

167 The S1 calculations show that our base results are insensitive to the value of P employed at V ≤ 5ms⁻¹
168 ¹; we get the same results regardless of whether we employ the lowest value (1.39) or the highest
169 value (1.66) Gong et al. [2002] reported based on calculations in the North Pacific and South
170 Pacific respectively. Furthermore, the S2 and S3 calculations show that our results are reasonably
171 robust to changes in the value of V at which we switch from P=1.39 to P=3.41, changing by less
172 than or similar to 10% upon increasing or decreasing this by 1ms⁻¹.

173

174 The effect of removing the [C]_{MBL} seasonality in the S4 calculations is variable, depending on the
175 model data used and the degree to which these are temporally averaged. Mostly, it has a modest
176 effect (of the order of 10%), however it has a more pronounced effect in the calculations with IPSL-
177 CM4 and HadAM3 climatological monthly-mean data. The change in δ¹³CH₄ we calculate could

178 therefore be sensitive to the assumed $[Cl_{MBL}]$ seasonality; we have employed the same $[Cl_{MBL}]$
179 seasonality as Allan et al. [2007], reflecting that of the radiation required to photolyse BrCl and Cl₂;
180 see equation 7 and accompanying text.

181

182 Finally, based on the S5 calculations, it would appear that the changes in temperature between the
183 PIH and LGM are responsible for a depletion in $\delta^{13}CH_4$ of approximately 0.05-0.1‰, depending on
184 the model data employed. The depletion reflects a reduction in the rate of reaction between Cl_{MBL}
185 and CH₄ due to the reduction in temperatures at the LGM (see Figure 1 and equation 5), only
186 marginally offset by an increase in the fractionation coefficient associated with this reaction (see
187 equation 4).

188

189

190 **4. Discussion**

191

192 Our calculations suggest circulation-driven changes in the strength of the Cl_{MBL} sink could have a
193 small but significant effect on $\delta^{13}CH_4$ on glacial-interglacial timescales. Depending on the model
194 data employed, and the degree to which these are temporally averaged, we calculate changes in
195 $\delta^{13}CH_4$ ranging from a depletion of 0.46‰ to an enrichment of 0.14‰, the magnitudes of which are
196 of the order of 10% of the 3.5‰ glacial-interglacial difference observed [Fischer et al., 2008].

197 Factors not explored here, which could have also affected $[Cl_{MBL}]$ and hence $\delta^{13}CH_4$ on these
198 timescales, include: changes in the lifetime of SSA (e.g. due to changes in precipitation); changes in
199 the acidity of the atmosphere (e.g. due to changes in DMS production linked to changes in biology,
200 such as plankton type and/or abundance); and changes in the intensity of radiation required to
201 photolyse BrCl and Cl₂ (e.g. due to changes in stratospheric ozone). $\delta^{13}CH_4$ could have also been
202 affected by changes in F_{Cl} (and F_{soil}) accompanying changes in F_{OH} , also not explored here. If
203 $F_{OH}=0.9$, $F_{soil}=0.06$ and $F_{Cl}=0.04$, and $\alpha_{OH}=1.0039‰$, $\alpha_{soil}=1.02‰$ and $\alpha_{Cl}=1.06‰$, a 5% increase

204 (decrease) in F_{OH} would lead to a 1.4‰ depletion (enrichment) in $\delta^{13}CH_4$ (assuming the change in
205 F_{OH} is compensated for by changes in F_{soil} and F_{Cl} , and $F_{Cl} = \frac{2}{3} F_{soil}$).

206

207 It is interesting that all of our calculations based on climatological monthly-mean data—arguably
208 the most robust—suggest that the circulation-driven changes in the Cl_{MBL} sink would have led to a
209 depletion in $\delta^{13}CH_4$ at the LGM relative to the PIH, primarily due to a reduction in the global
210 abundance of Cl_{MBL} . Ice-core records show an increase in sea salt at the LGM, by a factor of 15 in
211 the Arctic and 3 in the Antarctic [see Fischer et al., 2007, and references contained therein], which
212 we would expect to have been accompanied by proportional increases in $[Cl_{MBL}]$. Of course, there
213 could have been more Cl_{MBL} in polar regions but less at lower latitudes, yielding an overall
214 reduction. However, our calculations yield percentage increases in $[Cl_{MBL}]$ in some regions of the
215 Arctic Ocean approaching, but still short of, the 15-fold increase we would expect, and generally
216 capture less of the 3-fold increase expected in the Southern Ocean; see Figure 1. The calculations
217 based on CCSM3 and HadAM3 data yield increases limited to the regions south of about 50°S and
218 60°S, respectively, accompanied by decreases to the north of these, whilst the remainder of the
219 calculations predominantly show decreases in the Southern Ocean. This raises the question, what
220 SSA source are we missing or underestimating in our calculations, and what influence does it have
221 on $\delta^{13}CH_4$?

222

223 One possibility is that the simulations of the LGM circulation simply underestimate the wind speeds
224 at high latitudes. If this were the case, it could call into question the validity of these simulations in
225 other regions too. It certainly seems likely that at least part of the glacial-interglacial difference in
226 sea salt (and dust) was the result of changes in wind speeds governing the strength of sea-salt
227 sources, changes in wind patterns determining the efficiency of transport to Arctic and Antarctic
228 ice-core sites and/or changes in precipitation affecting its atmospheric lifetime [see, e.g., Fischer et
229 al., 2007; Petit et al., 2009]. However, there is some evidence that sea ice, as opposed to open

230 ocean, is the dominant source of SSA reaching both coastal and continental Antarctic sites [e.g.
231 Wagenbach et al., 1998; Rankin et al., 2002; Wolff et al., 2003, 2006]. In our calculations, we have
232 assumed that sea ice is an equally strong source, showing the same dependence on wind speed. If
233 however, sea ice were a stronger source on a per-unit-area basis, the increase in sea-ice at the LGM
234 could have contributed to the 3-fold increase in sea salt seen in the Antarctic, and perhaps the 15-
235 fold increase seen in the Arctic. A sea-ice driven increase in SSA, and hence Cl_{MBL} , at high
236 latitudes would tend to strengthen the Cl_{MBL} sink, and hence enrich $\delta^{13}CH_4$ at the LGM. However,
237 without knowing quantitatively how the strengths of the sea-ice and open-ocean sources compare,
238 we cannot say what the net effect on $\delta^{13}CH_4$ would be if the increase in sea-ice were factored into
239 our calculations.

240

241 What we can say is, irrespective of whether the net effect amounts to an enrichment or a depletion
242 in $\delta^{13}CH_4$, a change in $\delta^{13}CH_4$ due to a change in the strength of the Cl_{MBL} sink would have
243 implications for our interpretation of the glacial-interglacial $\delta^{13}CH_4$ record, and we have shown that
244 $\delta^{13}CH_4$ is affected non-negligibly by circulation-driven changes alone. Fischer et al. [2008]
245 attributed the enrichment in $\delta^{13}CH_4$ at the LGM to a near-complete shutdown of boreal wetland
246 sources of relatively ^{13}C -poor CH_4 , whilst biomass-burning sources of relatively ^{13}C -rich CH_4 were
247 little or unchanged relative to the pre-boreal Holocene (10 kyr BP). A global synthesis of charcoal
248 records by Power et al. [2008], however, has since shown that the last glacial period (16-21 kyr BP)
249 was the period of least biomass burning in the last 21 kyr, suggesting we still have some enrichment
250 in $\delta^{13}CH_4$ at the LGM to explain. An enrichment due to a strengthening of the Cl_{MBL} sink could
251 potentially contribute to this, whilst a depletion due to a weakening of the Cl_{MBL} sink would further
252 suggest the explanation offered by Fischer et al. [2007] is incomplete. Based on the results to our
253 calculations, the influence that Cl_{MBL} has on $\delta^{13}CH_4$ cannot be ignored in future interpretations of
254 the glacial-interglacial $\delta^{13}CH_4$ record, and hence further research is needed to quantify past changes
255 in the strength of this sink, including those relating to changes in the sea-ice source of SSA.

256

257

258 **Acknowledgements**

259

260 This work has been carried out as part of the British Antarctic Survey Polar Science for Planet Earth
261 programme. We gratefully acknowledge the funding of the Natural Environment Research Council.
262 The authors also wish to thank the PMIP2 international modeling groups for providing their data for
263 analysis, and the Laboratoire des Sciences du Climat et de l'Environnement (LSCE) for collecting
264 and archiving the model data. The PMIP2/MOTIF Data Archive is supported by CEA, CNRS, the
265 EU project MOTIF (EVK2-CT-2002-00153) and the Programme National d'Etude de la Dynamique
266 du Climat (PNEDC). The analyses were performed using version 10-13-2006 of the database. More
267 information is available on <http://pmip2.lsce.ipsl.fr>. Finally, we express our thanks to two
268 anonymous reviewers.

269

270

271 **References**

272

273 Allan, W., et al. (2005), Interannual variation of ^{13}C in tropospheric methane: Implications for a
274 possible atomic chlorine sink in the marine boundary layer, *J. Geophys. Res.*, 110, D11306,
275 doi:10.1029/2004JD005650.

276

277 Allan, W., et al. (2007), Methane carbon isotope effects caused by atomic chlorine in the marine
278 boundary layer: Global model results compared with Southern Hemisphere measurements, *J.*
279 *Geophys. Res.*, 112, D04306, doi:10.1029/2006JD007369.

280

281 Allan, W., et al. (2010), Modeling the effects of methane source changes on the seasonal cycles of
282 methane mixing ratio and $\delta^{13}\text{C}$ in Southern Hemisphere midlatitudes, *J. Geophys. Res.*, *115*,
283 D07301, doi:10.1029/2009JD012924.

284

285 Andreas, E. L. (1998), A New Sea Spray Generation Function for Wind Speeds up to 32 m s^{-1} , *J.*
286 *Phys. Oceanography*, *28*, 2175-2184.

287

288 Ferretti, D. F., et al. (2005), Unexpected Changes to the Global Methane Budget over the Past 2000
289 Years, *Science*, *309*, 1714, doi:10.1126/science.1115193.

290

291 Fischer, H., et al. (2007), Glacial/interglacial changes in mineral dust and sea-salt records in polar
292 ice cores: sources, transport and deposition, *Rev. Geophys.*, *45*, RG1002.

293

294 Fischer, H., et al. (2008), Changing boreal methane sources and constant biomass burning during
295 the last termination, *Nature*, *452*, 864-867.

296

297 Fung, I., et al. (1991), 3-Dimensional model synthesis of the global methane cycle, *J. Geophys.*
298 *Res.*, *96*, D7, 13,033-13,065.

299

300 Gong, S. L., et al. (2002), Canadian Aerosol Module (CAM): A size-segregated simulation of
301 atmospheric aerosol processes for climate and air quality models 2. Global sea-salt aerosol and its
302 budgets, *J. Geophys. Res.*, *107*, D24, 4779, doi:10.1029/2001JD002004.

303

304 Hansson, M. E. (1994), The Renland ice core – A Northern Hemisphere record of aerosol
305 composition over 12,000 years, *Tellus B*, *46*, 5, 390-418.

306

307 Kaplan, J. O., et al. (2006), Role of methane and biogenic volatile organic compound sources in late
308 glacial and Holocene fluctuations of atmospheric methane concentrations, *Global Biogeochem.*
309 *Cycles*, 20, GB2016, doi:10.1029/2005GB002590.

310

311 Kim, S.-J., et al. (2003), A coupled climate model simulation of the Last Glacial Maximum, Part 1:
312 approach to equilibrium, *Clim. Dyn.*, 20, 635-661, doi:10.1007/s00382-002-0292-2.

313

314 Levy, H. (1971), Normal atmosphere: Large radical and formaldehyde concentrations predicted,
315 *Science*, 173, 141-143.

316

317 Lelieveld, J., et al. (1998), Changing concentration, lifetime and climate forcing of atmospheric
318 methane, *Tellus*, 50B, 128-150.

319

320 Louergue, L., et al. (2008), Orbital and millennial-scale features of atmospheric CH₄ over the past
321 800,000 years, *Letters to Nature*, *Nature*, 453, 383-386.

322

323 Monahan, E. C., et al. (1986), A model of marine aerosol generation via whitecaps and wave
324 disruption, in *Oceanic Whitecaps and Their Role in Air-Sea Exchange Processes*, edited by E.C.
325 Monahan and G. MacNiocaill, Springer, New York, 167-174.

326

327 Petit J. R., et al. (1981), Ice age aerosol content from East Antarctic ice core samples and past wind
328 strength, *Nature*, 293, 391-394.

329

330 Petit, J. R., and B. Delmonte (2009), A model for large glacial–interglacial climate-induced changes
331 in dust and sea salt concentrations in deep ice cores (central Antarctica): palaeoclimatic
332 implications and prospects for refining ice core chronologies, *Tellus*, 61B, 768–790.

333

334 Platt, U., et al. (2004), Hemispheric average Cl atom concentration from $^{13}\text{C}/^{12}\text{C}$ ratios in
335 atmospheric methane, *Atmos. Chem. Phys.*, 4, 2393-2399.

336

337 Power, M. J., et al. (2008), Changes in fire regimes since the Last Glacial Maximum: an assessment
338 based on a global synthesis and analysis of charcoal data, *Clim. Dyn.*, 30, 887-907,
339 doi:10.1007/s00382-007-0334-x.

340

341 Rankin, A. M., et al. (2002), Frost flowers: implications for tropospheric chemistry and ice core
342 interpretation, *J. Geophys. Res.*, 107, 4683, doi:10.1029/2002JD002492.

343

344 Reeburgh, W. S., et al. (1997), Carbon kinetic isotope effect accompanying microbial oxidation of
345 methane in boreal forest soils, *Geochimica et Cosmochimica Acta*, 61, 22, 4761-4767.

346

347 Ridgwell, A. J., et al. (1999), Consumption of atmospheric methane by soils: A process-based
348 model, *Glob. Biogeochem. Cycles*, 13, 1, 59-70.

349

350 Röthlisberger, R., et al. (2002), Dust and sea salt variability in central East Antarctica (Dome C)
351 over the last 45kyrs and its implications for southern high-latitude climate, *Geophys. Res. Lett.*, 29,
352 20, 1963-1966, doi:10.1029/2002GL015186.

353

354 Sander, S. P., et al. (2003), Chemical Kinetics and Photochemical Data for Use in Atmospheric
355 Studies, Jet Propulsion Laboratory, JPL publication 02-25.

356

357 Saueressig, G., et al. (1995), Carbon kinetic isotope effect in the reaction of CH_4 with Cl atoms,
358 *Geophys. Res. Lett.*, 22, 1225-1228.

359

360 Saueressig, G., et al. (2001), Carbon 13 and D kinetic isotope effects in the reactions of CH₄ with
361 O(¹D) and OH: New laboratory measurements and their implications for the isotopic composition of
362 stratospheric methane, *J. Geophys. Res.*, 106, D19, 23,127-23,138.

363

364 Schaefer, H., and M. J. Whiticar (2008), Potential glacial-interglacial changes in stable carbon
365 isotope ratios of methane sources and sink fractionation, *Glob. Biogeochem. Cycles*, 22, GB1001,
366 doi:10.1029/2006GB002889.

367

368 Shin, S.-I., et al. (2003), A simulation of the Last Glacial Maximum climate using the NCAR-
369 CCSM, *Clim. Dyn.*, 20, doi:10.1007/s00382-002-0260-x, 127-151.

370

371 Snover, A. K., and P. D. Quay (2000), Hydrogen and carbon kinetic isotope effects during soil
372 uptake of atmospheric methane, *Glob. Biogeochem. Cycles*, 14, 1, 25-39.

373

374 Thompson, L. G. and E. Moseley-Thompson (1981), Microparticle concentration variations linked
375 with climatic change: Evidence from polar ice cores, *Science*, 212, 812-815.

376

377 Toggweiler, J. R. (1999), Variation of atmospheric CO₂ by ventilation of the ocean's deepest water,
378 *Paleoceanography*, 14, 5, 571-588.

379

380 Toggweiler, J. R., and J. Russell (2008), Ocean circulation in a warming climate, *Nature*, 451, 7176,
381 286-288.

382

383 Valdes, P. J., et al. (2005), The ice age methane budget, *Geophys. Res. Lett.*, 32, L02704,
384 doi:10.1029/2004GL021004.

385

386 Vogt, R., et al. (1996), A mechanism for halogen release from sea-salt aerosol in the remote marine
387 boundary layer, *Nature*, 383, 6598, 327-330.

388

389 Wagenbach, D., et al. (1998), Seasalt aerosol in coastal Antarctic regions, *J. Geophys. Res.*, 103,
390 10961-10974.

391

392 Witek, M. L., et al. (2007), Global sea-salt modelling: Results and validation against multicampaign
393 shipboard measurements, *J. Geophys. Res.*, 112, D08215, doi:10.1029/2006JD007779.

394

395 Wolff, E. W., et al. (2003), An ice core indicator of Antarctic sea ice production?, *Geophys. Res.*
396 *Lett.*, 30, 22, 2158-2161, doi:10.1029/2003GL018454.

397

398 Wolff, E. W., et al. (2006), Southern-Ocean sea-ice extent, productivity and iron flux over the past
399 eight glacial cycles, *Nature*, 440, doi:10.1038/nature04614.

400

Wind and temperature data

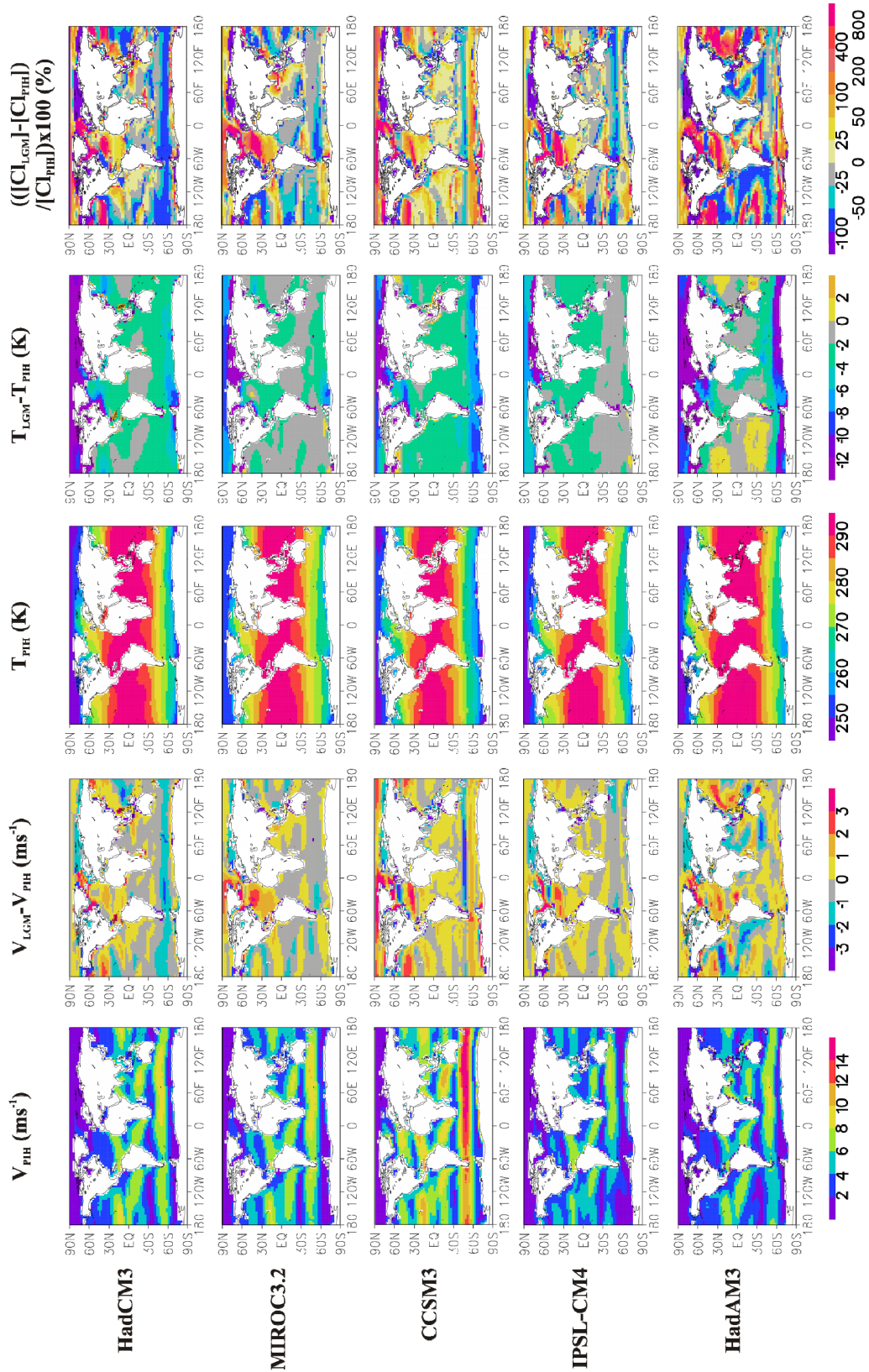
Model	Resolution	Data	'Temporal averaging'
HadCM3	3.75°lon x 2.5°lat; 19 levels	10m winds; 1.5m temperatures	Climatological monthly means based on 100-year integrations
MIROC3.2	2.8°lon x 2.8°lat; 20 levels	10m winds; 2m temperatures	Climatological monthly means based on 100-year integrations
CCSM3	2.8°lon x 2.8°lat; 26 levels	1000mb winds and temperatures*	Climatological monthly means based on 100-year integrations (& 100 years of monthly means)
IPSL-CM4	3.75°lon x 2.5°lat; 19 levels	10m winds; 1.5m temperatures	Climatological monthly means based on 100-year integrations
HadAM3	3.75°lon x 2.5°lat; 19 levels	10m winds; 997mb temperatures	Climatological monthly means based on 20-year integrations (& 20 years of daily means)

Table 1. Main features of the data on which our calculations are based. *The wind and temperature data from CCSM3 correspond to the winds and temperatures on the lowest model level: mostly 1000mb, but in places 925mb or 850mb.

Changes in $\delta^{13}\text{CH}_4$

Model	B	S1	S2	S3	S4	S5
HadCM3	-0.46	-0.46	-0.44	-0.51	-0.39	-0.38
MIROC3.2	-0.25	-0.25	-0.24	-0.28	-0.22	-0.19
CCSM3	-0.15 (-0.22)	-0.15 (-0.22)	-0.15 (-0.23)	-0.14 (-0.22)	-0.13 (-0.22)	-0.02 (-0.10)
IPSL-CM4	-0.23	-0.23	-0.20	-0.26	-0.13	-0.15
HadAM3	-0.24 (0.14)	-0.24 (0.14)	-0.22 (0.14)	-0.25 (0.16)	-0.07 (0.12)	-0.17 (0.22)

Table 2. Changes in $\delta^{13}\text{CH}_4$ (‰) calculated in the base (B) and sensitivity (S1-5) calculations; the numbers in parentheses correspond to the results obtained when less 'temporally averaged' data are employed (see Table 1 and accompanying text for details).



414

415 **Figure 1.** Annual-mean surface wind speeds (V_{PIH}) and temperatures (T_{PIH}) in the PIH, and the changes in these at the
 416 LGM ($V_{LGM} - V_{PIH}$ and $T_{LGM} - T_{PIH}$), based on the climatological monthly-mean data from each model. Also, the
 417 percentage changes in $[Cl_{MBL}]$ that we calculate at the LGM ($\frac{([Cl_{MBL}]_{LGM} - [Cl_{MBL}]_{PIH})}{[Cl_{MBL}]_{PIH}} \times 100$) based on
 418 the wind data.